Subwavelength beam manipulation via multiple-metal slits coupled by disk-shaped nanocavity*

Zheng Gai-Ge(郑改革)†, Xu Lin-Hua(徐林华), Pei Shi-Xin(裴世鑫), and Chen Yun-Yun(陈云云)

School of Physics and Optoelectronic Engineering, Nanjing University of Information Science & Technology, Nanjing 210044, *China*

(Received 23 May 2013; revised manuscript received 15 July 2013; published online 12 February 2014)

A novel plasmonic structure consisting of three nano-scaled slits coupled by nano-disk-shaped nanocavities is proposed to produce subwavelength focusing and beam bending at optical frequencies. The incident light passes through the metal slits in the form of surface plasmon polaritons (SPPs) and then scatters into radiation fields. Numerical simulations using finite-difference time-domain (FDTD) method show that the transmitted fields through the design example can generate light focusing and deflection by altering the refractive index of the coupled nanocavity. The simulation results indicate that the focal spot is beyond the diffraction limit. Light impinges on the surface at an angle to the optical axis will add an extra planar phase front that interferes with the asymmetric phase front of the plasmonic lens, leading to a larger bending angle off the axial direction. The advantages of the proposed plasmonic lens are smaller device size and ease of fabrication. Such geometries offer the potential to be controlled by using nano-positioning systems for applications in dynamic beam shaping and scanning on the nanoscale.

Keywords: beam manipulation, surface plasmon, subwavelength slits

PACS: 42.79.Fm, 42.25.−p, 78.68.+m **DOI:** 10.1088/1674-1056/23/3/034213

1. Introduction

Surface plasmon polaritons (SPPs) are surface electromagnetic (EM) waves propagating along the interface of metal and dielectric, and their amplitudes decay exponentially from the interface.[1] They play a central role in the field of nanophotonics and have drawn considerable attention in recent years.[2–4] The most attractive feature of SPPs is the ability of manipulating light on a subwavelength scale with resonant field enhancement.[5–7] Therefore, there is a growing interest in developing plasmonic structures. Plasmonic lenses with different geometries, including circular holes with concentric grooves,[8] slits flanked by linear arrays of grooves,[9] metal slits with variant depths[10] or widths,[11–15] and single metallic slit surrounded by grooves,[16–18] have been designed and developed to replace conventional dielectric-based lenses for the ability to manipulate and control light on a subwavelength scale. Recently, Zhao *et al.* proposed that different types of plasmonic lenses can not only focus, but also bend EM waves.[19] The bending effect was achieved by constructing an asymmetric phase front caused by varying phase retardations in EM waves. However, for certain applications, it would be highly desirable to realize positional modulation through a plasmonic lens without changing the period of array, or the length and width of slits. Complex structures and sophisticated parameters make them especially difficult to fabricate by using the present techniques.

In this paper, we design a plasmonic structure to realize sub-wavelength beam focusing and bending. The structure consists of metal slits with the same width and interval with side coupled disk-shaped nanocavities. The focusing and bending effects are achieved by constructing a symmetric and an asymmetric phase front caused by varying phase retardations in EM waves as they pass through the multiple-metal slits. There is no need to change the period of array, the length and width of the slits. Thus, the structure proposed is smaller, more compact, and convenient for integration. The finite-difference time-domain (FDTD) method is employed to verify the proposed designs. The simulation results indicate the proposed lens can yield a converging beam with a focal spot size beyond the diffraction limit. The proposed structure can also allow effective beam bending under both normal and tilted incidence. Compared with other existing counterparts, the structure proposed in this work has the advantages of small focal spot size, simple structure, and compact dimension.

2. Design and simulation method

Figure 1 shows the schematic of the designed plasmonic lens which consists of three metallic slits symmetrically arranged along the z direction. The metallic slits have the same widths and intervals. When the incident light illuminates the left side of the structure, the light wave is coupled to SPP modes at the entrances of the metallic slits and propagates

*Project supported by the National Natural Science Foundation of China (Grant No. 61203211), the Natural Science Foundation of Jiangsu Higher Education Institutions of China (Grant No. 13KJB140006), and the Foundation for Outstanding Young Teachers of Nanjing University of Information Science & Technology, China (Grant No. 20110423).

†Corresponding author. E-mail: eriot@126.com

© 2014 Chinese Physical Society and IOP Publishing Ltd

along the slits. After transferring to the ends of the metallic slits, the SPPs will be converted to radiating fields due to the scattering of the structure surface. There are two SPP modes in the metallic slit, which are the symmetric mode and the anti-symmetric mode with its H-field distributions. In the sub-wavelength slit, only the symmetric mode exists, but the anti-symmetric mode undergoes cut-off. From the Maxwell's equations and boundary conditions, the complex propagation constant β of the fundamental SPP mode is given by[11]

$$\tanh\left(\frac{w}{2}\sqrt{\beta^2-\varepsilon_{\rm d}k_0^2}\right)=\frac{-\varepsilon_{\rm d}\sqrt{\beta^2-\varepsilon_{\rm m}k_0^2}}{\varepsilon_{\rm m}\sqrt{\beta^2-\varepsilon_{\rm d}k_0^2}}, \tag{1}$$

where k_0 is the wave number in the free space, w is the slit width, $\varepsilon_{\rm d}$ and $\varepsilon_{\rm m}$ are the relative dielectric constants for metal and the materials between slits, respectively. The effective index $n_{\rm eff}$ of MDM waveguide as a function of wavelength can be calculated by $n_{\rm eff}=\beta/k_0$. We have known that the complex wave number gradually decreases as the slit width increases. If the slit width goes to infinity, β approaches the propagation constant in the air.[11]

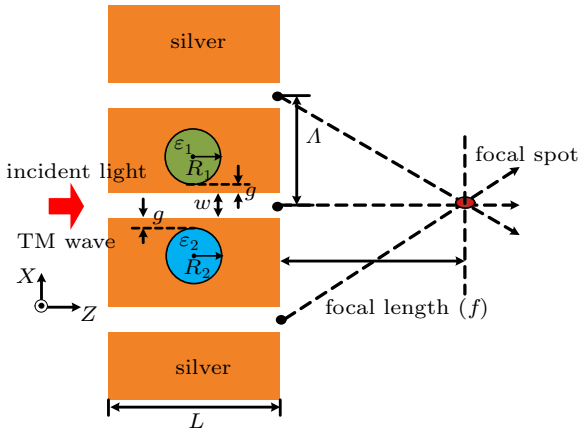


Fig. 1. (color online) Schematic diagram of the proposed plasmonic lenses. A metal slit array is embedded in the metal slab coupled with a disk-shaped cavity. The thickness of the structure is L, and the slit interspacing (center to center) is Λ, while each slit width is w. The g represents the gap distance, R_1 and R_2 are the radii of the introduced ring resonators. A transverse magnetic light is incident from the left of the metal slab.

In the calculation, the dielectric function of metal is described by the following Drude model:

$$\varepsilon_{\rm Ag}(\omega)=\varepsilon_\infty-\frac{\omega_{\rm p}^2}{\omega^2+{\rm i}\gamma\omega}, \tag{2}$$

where ε_∞ is the infinite frequency dielectric constant, $\omega_{\rm p}$ is the bulk plasma frequency, ω is the angular frequency, and γ the collision frequency which is related to the dissipation loss in the metal. These parameters are set to be 6.0, 1.5×10^{16} rad/s, and 7.73×10^{13} rad/s, respectively.[20] We assume that the monochromatic operation with the free space wave number $k_0=\omega_0/c$, the time dependence of $\exp(-{\rm j}\omega t)$, and the corresponding free space wave length $\lambda_0=2\pi/k_0$. Here, c is the speed of light in vacuum.

To demonstrate the validity of the designed structure, two-dimensional FDTD simulation is performed with the perfectly matched layer (PML) absorbing boundary conditions in x and z directions of the simulation domain. Since the width of the bus waveguide is much smaller than the operating wavelength in the structure, only the fundamental waveguide mode is supported. The incident light for excitation of the SPP mode is a TM-polarized (the magnetic field is parallel to the y axis) fundamental mode. In the following FDTD simulations, the grid sizes in the x and z directions are chosen to be $\Delta x=\Delta z=2$ nm and $\Delta t=\Delta x/2c$, which are sufficient for the numerical convergence. The normalized time-averaged magnetic field intensity $|H_y|^2$ is employed to represent the field intensity.

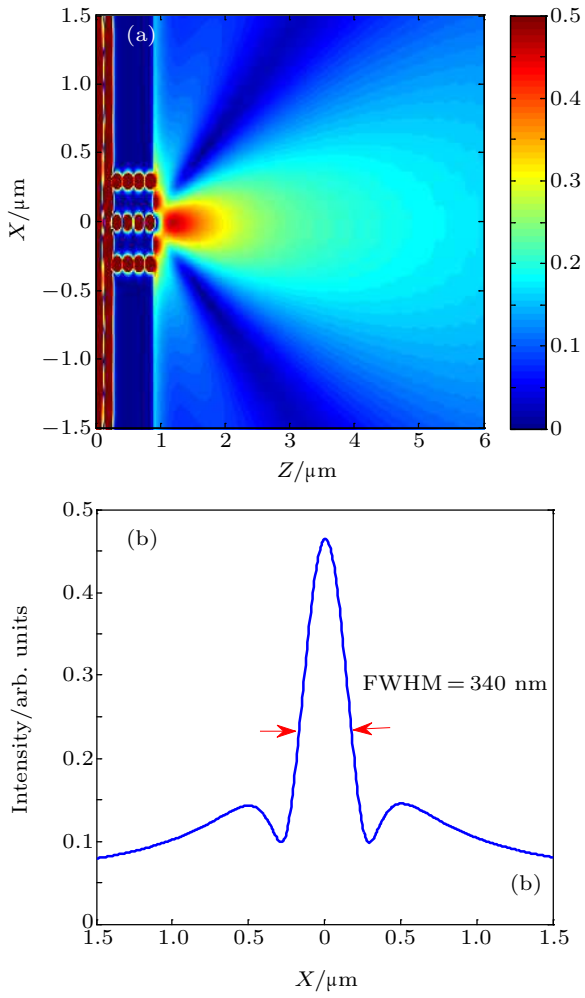


Fig. 2. (color online) (a) The field intensity distribution of the transmitted lights through the plasmonic structure. (b) The cross-section at the focal point along the x axis.

In the three-slits based waveguide array, each radiating field at the ends of the metallic slits can be regarded as an individual point source, while propagation is in the shape of a

spherical wave from the sources into the air. They are focused at the specific point due to the constructive interference. Figure 2 shows the intensity distribution with a focal length f of 0.35 μm and full width at half maximum (FWHM) of 340 nm when 500-nm light is incident normally on the metallic surface. The simulation parameters are chosen as $L = 670$ nm, $\Lambda = 300$ nm, $w = 50$ nm, and $g = 20$ nm. An important point of simulation results is that the focal length can be smaller than the wavelength and the cross section of the focus spot can be narrower than the incident wavelength.

3. Subwavelength focusing with the coupled cavity

Many excellent studies about the metallic nanolens have been reported.[8–11,17,18,21,22] Kim proposed a method for optical beam focusing by a single subwavelength metal slit surrounded by chirped surface gratings.[21] The device requires six dielectric gratings on each side of a single metal slit to perform the beam focusing. The FWHM of the focal spot is a little narrower than the incident wavelength. A metallic lens comprising of specially designed nanoslits formed on the silver slab has also been proposed by Xu *et al.*[22] Although this structure can be used to achieve subwavelength focusing, many slits perforated in the silver slab have to be designed with variant widths to produce the desired optical phase retardations. To overcome these limitations, we will introduce a much simpler subwavelength focusing method through the application of a cavity coupled plasmonic waveguide array.

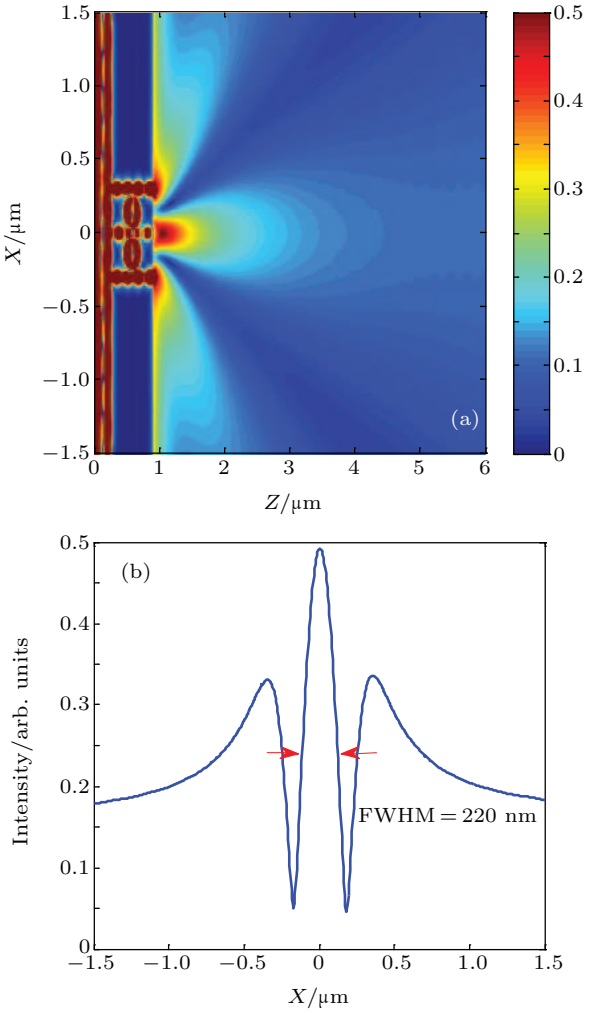


Fig. 3. (color online) (a) Light field intensity distribution of the transmitted light through the designed lens coupled with disk-shaped cavity. (b) Cross-section along the x direction at focal spot.

To demonstrate the validity of designed structure, two-dimensional FDTD simulation is performed. The parameters of our structure are set as follows: $\varepsilon_1 = \varepsilon_2 = 1$, and $R_1 = R_2 = 100$ nm. The other parameters are the same as that in Fig. 2. The simulation result displayed in Fig. 3(a) proves that a focal spot is produced in near field as expected. From the figure, a clear-cut focus appears at about 185 nm away from the exit surface. Because of the metal slits with equal width and depth, the difference of phase retardations between slits will not be generated when the SPPs are propagating at the metal slits zone. After introducing nanocavities, the intensity distributions of the SP wave will be changed, which can be observed by comparing Fig. 2(a) and Fig. 3(a). The cross section of the focus spot in the x direction is shown in Fig. 3(b), indicating an FWHM of 220 nm, which is beyond the diffraction limit. The choice of parameters making the multi-slits can be easily fabricated by focused ion beams (FIB) in the experiment.

4. Beam bending controlled by side-coupled cavity

To fully realize the potential of plasmonic lenses, it is necessary to not only focus light, but also to manipulate and precisely position it at small scales. In Ref. [19], plasmonic lenses that can not only focus, but also bend electromagnetic (EM) waves have been designed and characterized. The control of the phase front profile is achieved through two mechanisms: phase retardation caused by the width and shape of the individual slits in the lens, and the position of these slits. For certain applications, it would be highly desirable to realize positional modulation through a plasmonic lens without changing the period of array, or the length and width of slits. To deflect the beam, a curved phase front of the transmitted beam should be achieved. Phase retardation in our structure is tuned by the introduced cavity in our design (see Fig. 4). The position of focus and the bending angle are determined using the image processing software (Image J), to capture the area with the highest intensity within the main beam.

Figures 5(a)–5(d) further illustrate the corresponding H-field intensity distributions for four different values of ε. The H-field intensity distribution shows that the energy emerging from the structure tends to focus within several micrometers in an extremely small region. Under normally incident radiation

with a wavelength of 500 nm, a plane TM wave incident from the left side is deflected by an angle to the top of the original propagation direction. When the refractive index of the material that fills in the cavity changes, the deflection angle can be controlled. For example, the case of $\varepsilon = 1.2$ shown in Fig. 5(a) reveals a deflection angle of 2.3°. When ε_1 increases to 1.4, the deflection angle increases to 4.5° (see Fig. 5(b)). For the case of $\varepsilon = 1.8$, the deflection angle increases to 6.2° (see Fig. 5(c)). When $\varepsilon = 2.0$, the deflection angle changes to 10.8° (see Fig. 5(d)). In addition, the four designs vary not only in bending angle, but also in light distribution and intensity. The intensity of focal spot decreases with increasing ε.

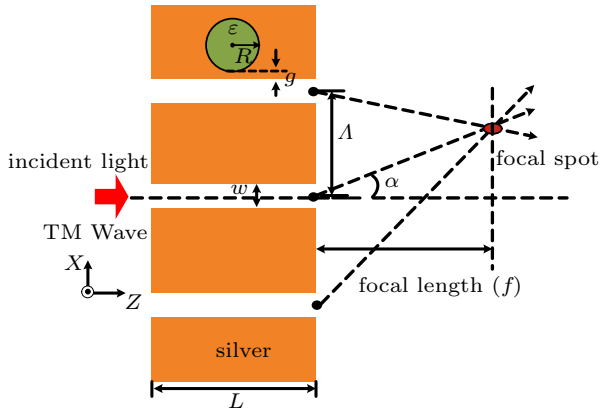


Fig. 4. (color online) Schematic of a plasmonic lens that can bend a light beam or focal point in the transverse direction.

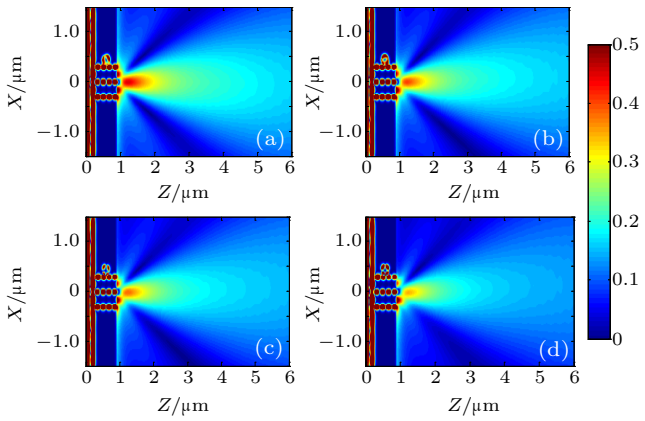


Fig. 5. (color online) Simulated magnetic field profiles of the single-disk coupled plasmonic lens with different refractive indices. (a) $\varepsilon = 1.2$, (b) $\varepsilon = 1.4$, (c) $\varepsilon = 1.8$, and (d) $\varepsilon = 2.0$.

As shown in Fig. 5, the incident light is normal to the lens surface. We proceed to investigate the lens performance when the EM waves are incident at an angle to the optical axis (Fig. 6). Light impinges on the left surface at an angle of θ to the optical axis ($z = 0$). Such a condition adds an extra planar phase front that interferes with the asymmetric phase front of the plasmonic lens, leading to a larger bending angle off the axial direction. Figures 7(a)–7(c) show that the bending angle increases from 10.4° to 16° when the incident angle changes from 5° to 20°. Moreover, our simulation results also indicate that when the incident angle is 50° (Fig. 7(d)), one cannot observe the focal spot any more.

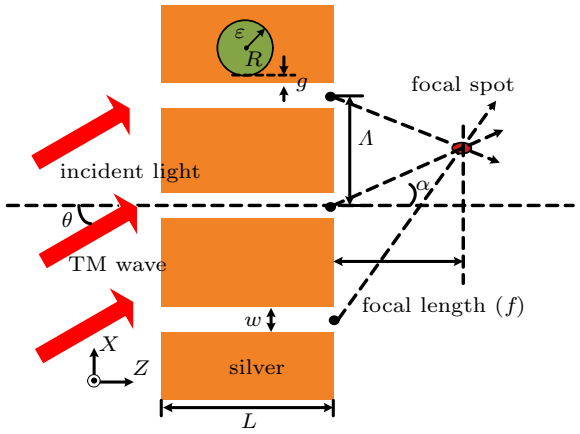


Fig. 6. (color online) Schematic diagram of the proposed plasmonic lenses. A transverse magnetic (TM) light is incident on the left side of the metal slab with an angle of θ.

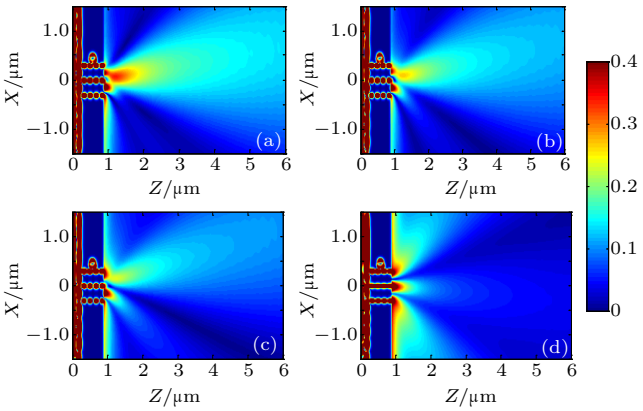


Fig. 7. (color online) Influence of incident angles on the bending effects. (a)–(d) Simulation results corresponding to the case that the light is incident at an angle of 10°, 15°, 20°, and 50° to the optical axis, respectively.

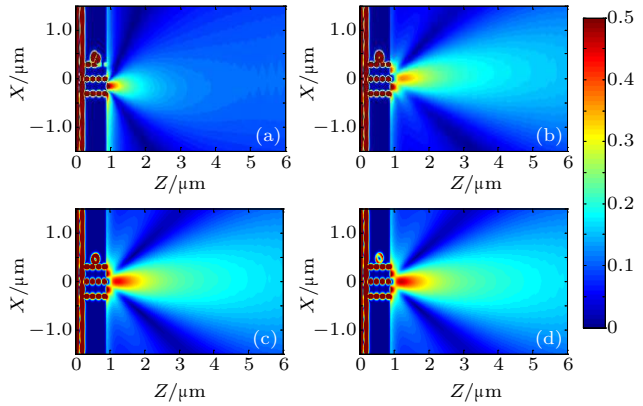


Fig. 8. (color online) Influence of gap distances on the bending effects. (a)–(d) Simulation results corresponding to the cases of $g = 10$ nm, $g = 20$ nm, g =30 nm, and g =50 nm, respectively.

When the incident light with an angle of θ illuminates the left side of the structure, the light wave is coupled to SPP modes at the entrances of the metallic slits and propagates

along the slits. After transferring to the ends of the metallic slits, the SPPs will be converted to radiation fields due to the scattering of the structure surface. The multiple-beam constructive interference should occur if the phase difference between the light radiated from different slits at the focusing spot position is equal to $2m\pi$ ($m = \pm 1, 2, 3 \ldots$). In fact, no constructive interferences occur after θ increases to a certain value, and the critical angle is calculated to be 37° in this model.

In previous calculations, the gap distance (g) is fixed. Figures 8(a)–8(d) show that the bending angle changes when g increases from 10 nm to 50 nm. As illustrated in Figs. 8(c) and 8(d), g has less influence on the bending effect because nearly all of SPPS can be transmitted.

5. Discussion

Although some excellent designs of metal slit arrays are capable of focusing light beyond the diffraction limit, most of the structures consist of metal slits with different widths and intervals, complex structures and sophisticated parameters, which make them especially difficult to fabricate. The advantages of our proposed plasmonic lens are smaller device size and ease of fabrication. The simulation results clearly show that the deflection angle and the focal spot size can be controlled by adjusting the parameters of the introduced nano-cavity.

For beam deflection at a specific angle α, overall phase retardation of the system of several slits embedded in the metal layer is[23]

$$\phi(x) = 2m\pi + \phi(0) - \frac{2\pi}{\lambda_0} x \sin(\alpha), \tag{3}$$

where x is the direction normal to the surface of the metal, λ_0 is the wavelength of free space, and m is an integer. Thus, the most important step for beam deflection from a plasmonic device involves a careful optimization of the overall phase retardation. In that sense, introducing the nano-cavity coupled with the nano-slits in our systems is equivalent to changing the effective index of each slit. Owing to the fact that the transmittance of the slit depends on the effective index of the slits, the amplitude and phase of the transmittance change for each slit, thus modifying the beam manipulation of the overall system. When the SPPs arrive at the nano-cavity zone, the different waveguide would introduce different phase retardation among the radiation components at the exit surface of slot wavelengths and result in beam deflection.

Recently, some methods for active plasmonic devices have been proposed, such as thermo-optic mechanism,[24] electro-optic mechanism,[25,26] adoption of photo-chromic molecules,[27] nonlinear effects,[28–31] and so on. Among these, using optical nonlinear effects is an attractive approach for active control of optical signal in plasmonic devices because those nonlinear materials can operate in an all-optical means with an ultra-fast response time. The transmission characteristics of MDM waveguide coupling to a nano-disk cavity filled with a Kerr nonlinear material can be tuned with an external control (pumping) beam. In our design, the cavity can also be filled with nonlinear materials, then the deflection angle can be controlled by the intensity of incident light. It is assumed that the intensity-dependent index change in the stub is completely governed by the third-order optical nonlinearity of material. The subwavelength slit is coupled to one stub filled with Kerr medium whose dielectric constant depends on the intensity of incident light:[32]

$$\varepsilon_{\mathrm{d}} = \varepsilon_{\mathrm{l}} + \chi^{(3)} |E|^2, \tag{4}$$

where ε_{l} is the linear dielectric constant and set as 2.25, the third-order nonlinear susceptibility $\chi^{(3)}$ is chosen as a typical value of nonlinear optical materials such as indium tin oxide (ITO) thin film with $\chi^{(3)} = 1 \times 10^{-10}$ esu ($\approx 2.79 \times 10^{-18}$ m^2/V^2). The optical intensity is determined by $|E|^2$ which represents the amplitude (peak value) of the incident light and $|E|^2$ are chosen as 1 V^2/m^2 and 9×10^{16} V^2/m^2. The FDTD simulations of magnetic-field distribution at different incident intensities are shown in Figs. 9(a) and 9(b). By changing intensities of the incident light, the focal length, the FWHM of the focal width, and the bending angle can be adjusted. This relation implies a way of focusing modulation by changing the dielectric constant in the metallic slits, which can be implemented by embedding nonlinear material into the slits.

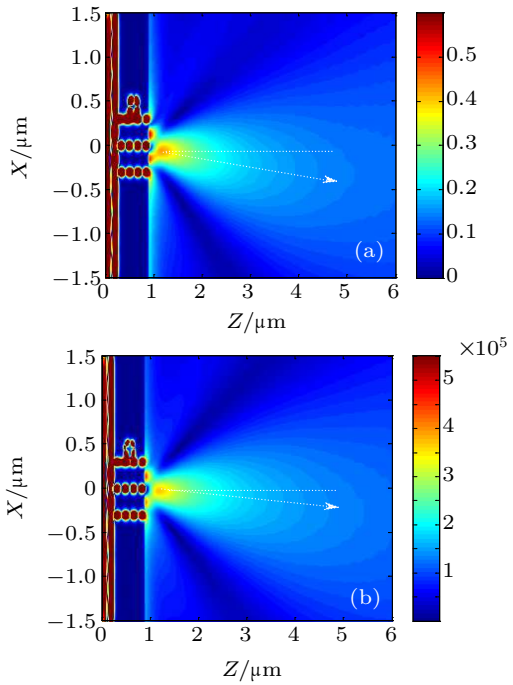


Fig. 9. (color online) Magnetic-field intensity distributions at different incident intensities when the stub is filled with Kerr nonlinear medium. (a) $|E|^2 = 1$ V^2/m^2; (b) $|E|^2 = 9 \times 10^{16}$ V^2/m^2. The other parameters are the same as that in Fig. 5.

Such dynamical control on the beam direction can lead to other applications of nano-lenses such as nano-scanners or can be exploited for high-density memory reading and writing. In combination with the previous ideas on active control of nano-lenses, we expect that our results could lead to the realization of optimum designs of nano-lenses. This should play an important role in arousing new experiments and applications in nanophotonics.

6. Conclusions

In summary, a plasmonic lens composed of metal nano-slits coupled by a dielectric disk-shaped cavity is proposed. Two main phenomena, optical beam deflection and focusing, are investigated numerically. The simulation results clearly show that the deflection angle and the focal spot size can be controlled by adjusting the parameters of cavities. The advantages of our proposed plasmonic lens include smaller device size and ease of integration. In combination with the ideas on active control of nano-lenses, we expect that our results could lead to the realization of optimum designs of nano-lenses.

References

[1] Zayats A V, Smolyaninovv I I and Maradudin A A 2005 *Phys. Rep.* **408** 131
[2] Barnes W L, Dereux A and Ebbesen T W 2003 *Nature* **424** 824
[3] Ozbay E 2006 *Science* **311** 189
[4] Wu C N, Li H J, Peng X, Cao G T and Liu Z M 2013 *Chin. Phys. B* **22** 057301
[5] Drezet A, Stepanov A L, Ditlbacher H, Hohenau A, Steinberger B, Aussenegg F R, Leitner A and Krenn J R 2005 *Appl. Phys. Lett.* **86** 074104
[6] Chen F X, Wang L S and Xu W Y 2013 *Chin. Phys. B* **22** 045202
[7] Griesing S, Englisch A and Uwe H 2008 *Opt. Lett.* **33** 575
[8] Yin L, Vlasko-Vlasov V K, Pearson J, Hiller J M, Hua J, Welp U, Brown D E and Kimball C W 2005 *Nano Lett.* **5** 1399
[9] López-Tejeira F, Rodrigo S G, Martín-Moreno L, García-Vidal F J, Devaux E, Ebbesen T W, Krenn J R, Radko I P, Bozhevolnyi S I, González M U, Weeber J C and Dereux A 2007 *Nat. Phys.* **3** 324
[10] Sun Z J and Kim H K 2004 *Appl. Phys. Lett.* **85** 642
[11] Shi H F, Wang C T, Du C L, Luo X G, Dong X C and Gao H T 2005 *Opt. Express* **13** 6815
[12] Zhu Q F, Wang D Y, Zheng X H and Zhang Y 2011 *Appl. Opt.* **50** 1879
[13] Yu Y T and Zappe H 2011 *Opt. Express* **19** 9434
[14] Li H, Yan L S, Guo Z, Pan W, Wen K H, Li H Y and Luo X G 2012 *IEEE Photon. J.* **4** 57
[15] Chen Q and Cumming D R 2010 *Opt. Express* **18** 14788
[16] Shi H F, Du C L and Luo X G 2007 *Appl. Phys. Lett.* **91** 093111
[17] Hao F H, Wang R and Wang J 2010 *Plasmonics* **5** 45
[18] Hao F H, Wang R and Wang J 2010 *Opt. Express* **18** 15741
[19] Zhao Y H, Lin S S, Nawaz A A, Kiraly B, Hao Q Z, Liu Y J and Huang T J 2010 *Opt. Express* **18** 23458
[20] Liu Z, Durant S, Lee H, Xiong Y, Pikus Y, Sun C and Zhang X 2007 *Opt. Lett.* **32** 629
[21] Kim S, Lim Y, Kim H, Park J and Lee B 2008 *Appl. Phys. Lett.* **92** 013103
[22] Xu T, Du C L, Wang C T and Luo X G 2007 *Appl. Phys. Lett.* **92** 201501
[23] Xu T, Wang C T, Du C L and Luo X G 2008 *Opt. Express* **16** 4753
[24] Lereu A L, Passian A, Goudonnet J P, Thundat T and Ferrell T L 2005 *Appl. Phys. Lett.* **86** 154101
[25] Dicken M J, Sweatlock L A, Pacifici D, Lezec H J, Bhattacharya K and Atwater H A 2008 *Nano Lett.* **8** 4048
[26] Hsiao K S, Zheng Y B, Juluri B K, Huang T J 2008 *Adv. Mater.* **20** 3528
[27] Pala R A, Shimizu K T, Melosh N A and Brongersma M L 2008 *Nano Lett.* **8** 1506
[28] Wurtz G A and Zayats A V 2008 *Laser Photon. Rev.* **2** 125
[29] Liu Y M, Bartal G, Genov D A and Zhang X 2007 *Phys. Rev. Lett.* **99** 153901
[30] Wurtz G A, Pollard R and Zayats A V 2006 *Phys. Rev. Lett.* **97** 057402
[31] Porto J A, Moreno L M and Garcia-Vidal F J 2004 *Phys. Rev. B* **70** 081402
[32] Min C J, Wang P, Chen C C, Deng Y, Lu Y H, Ming H, Ning T Y, Zhou Y L and Yang G Z 2008 *Opt. Lett.* **33** 869